

Generating Lookup Tables from the AE9/AP9 Models

June 16, 2015

Joshua P. Davis
Vehicle Concepts Department
Architecture and Design Subdivision

Prepared for:

Space and Missile Systems Center
Air Force Space Command
483 N. Aviation Blvd.
El Segundo, CA 90245-2808

Contract No. FA8802-14-C-0001

Authorized by: Engineering and Technology Group

Distribution Statement A: Approved for public release; distribution unlimited.

Report Documentation Page		Form Approved OMB No. 0704-0188
Public reporting burden for the collection of information is estimated to average 1 hour per response, including the time for reviewing instructions, searching existing data sources, gathering and maintaining the data needed, and completing and reviewing the collection of information. Send comments regarding this burden estimate or any other aspect of this collection of information, including suggestions for reducing this burden, to Washington Headquarters Services, Directorate for Information Operations and Reports, 1215 Jefferson Davis Highway, Suite 1204, Arlington VA 22202-4302. Respondents should be aware that notwithstanding any other provision of law, no person shall be subject to a penalty for failing to comply with a collection of information if it does not display a currently valid OMB control number.		
1. REPORT DATE 16 JUN 2015	2. REPORT TYPE Final	3. DATES COVERED -
4. TITLE AND SUBTITLE Generating Lookup Tables from the AE9/AP9 Models		5a. CONTRACT NUMBER FA8802-14-C-0001
		5b. GRANT NUMBER na
		5c. PROGRAM ELEMENT NUMBER 5811
6. AUTHOR(S) Joshua P. Davis		5d. PROJECT NUMBER 11
		5e. TASK NUMBER na
		5f. WORK UNIT NUMBER na
7. PERFORMING ORGANIZATION NAME(S) AND ADDRESS(ES) The Aerospace Corporation 2310 E. El Segundo Blvd. El Segundo, CA 90245-4609		8. PERFORMING ORGANIZATION REPORT NUMBER TOR-2015-00893
9. SPONSORING/MONITORING AGENCY NAME(S) AND ADDRESS(ES) Space and Missile Systems Center Air Force Space Command 483 N. Aviation Blvd. El Segundo, CA 90245		10. SPONSOR/MONITOR'S ACRONYM(S) SMC/AD
		11. SPONSOR/MONITOR'S REPORT NUMBER(S) na
12. DISTRIBUTION/AVAILABILITY STATEMENT Approved for public release, distribution unlimited		
13. SUPPLEMENTARY NOTES A companion report -- TOR-2016-00142 -- will be submitted soon that will include data tables related to this one (TOR-2015-00893)., The original document contains color images.		
14. ABSTRACT A method of generating a set of static lookup tables from AE9/AP9 data in order to reduce the analysis time required for quick results while maintaining a high degree of agreement between the lookup tables and the AE9/AP9 models is investigated. Multiple orbits ranging from a LEO Sun synchronous orbit at a 350 km altitude to a Tundra orbit were looked at to determine the agreement of the static lookup tables to the AE9/AP9 model software results. It was determined that, for the orbits used in the validation study, the static lookup tables provided small enough errors to be considered a viable alternative to the AE9/AP9 software for fast turn-around conceptual level analysis.		
15. SUBJECT TERMS Radiation Environment, AE9, AP9		

16. SECURITY CLASSIFICATION OF:			17. LIMITATION OF ABSTRACT UU	18. NUMBER OF PAGES 14	19a. NAME OF RESPONSIBLE PERSON
a. REPORT unclassified	b. ABSTRACT unclassified	c. THIS PAGE unclassified			

Abstract

A method of generating a set of static lookup tables from AE9/AP9 data in order to reduce the analysis time required for quick results while maintaining a high degree of agreement between the lookup tables and the AE9/AP9 models is investigated. Multiple orbits ranging from a low Earth orbit (LEO) sun-synchronous orbit at a 350-km altitude to a Tundra orbit were looked at to determine the agreement of the static lookup tables with the AE9/AP9 model software results. It was determined that, for the orbits used in the validation study, the static lookup tables provided small enough errors to consider them a viable alternative to the AE9/AP9 software for fast turnaround and conceptual-level analysis.

Acknowledgments

The author would like to acknowledge T. P. O'Brien, J. Padin, D. Y. Stodden, and J. M. Coggi for their help throughout this project.

Contents

1.	Introduction	1
2.	Method	1
3.	Validation Study.....	3
3.1	GEO Results.....	4
3.2	GIO Results	5
3.3	Tundra Orbit Results	7
3.4	Magic Orbit Results	8
3.5	Molniya Orbit Results	10
3.6	PNT Orbit Results	11
3.7	Sun Synchronous Orbit at 350 km Results.....	13
3.8	Sun Synchronous Orbit at 500 km Results.....	14
3.9	Sun Synchronous Orbit at 750 km Results.....	16
3.10	Sun Synchronous Orbit at 1500 km Results.....	17
3.11	Mid-Inclined LEO at 400 km	19
4.	Conclusion	20
5.	References	21

Figures

Figure 1.	Visualization of AE9 integral 1 MeV electrons using SOAP and a static 3D table containing data generated from the AE9/AP9 model.	2
Figure 2.	GEO integral electron fluence error.....	4
Figure 3.	GEO integral proton fluence error.	5
Figure 4.	GEO total dose error.	5
Figure 5.	GEO integral electron fluence error.....	6
Figure 6.	GEO integral proton fluence error.	6
Figure 7.	GEO total dose error.	7
Figure 8.	Tundra orbit integral electron fluence error.	7
Figure 9.	Tundra orbit integral proton fluence error.	8
Figure 10.	Tundra orbit total dose error.	8
Figure 11.	Magic orbit integral electron fluence error.	9
Figure 12.	Magic orbit integral proton fluence error.....	9
Figure 13.	Magic orbit total dose error.....	10
Figure 14.	Molniya orbit integral electron fluence error.....	10
Figure 15.	Molniya orbit integral proton fluence error.	11
Figure 16.	Molniya orbit total dose error.	11
Figure 17.	PNT orbit integral electron fluence error.....	12
Figure 18.	PNT orbit integral proton fluence error.	12
Figure 19.	PNT orbit total dose error.	13
Figure 20.	Sun-Synchronous orbit at 350 km integral electron fluence error.	13
Figure 21.	Sun-Synchronous orbit at 350 km integral proton fluence error.....	14
Figure 22.	Sun-Synchronous orbit at 350 km total dose error.	14
Figure 23.	Sun-Synchronous orbit at 500 km integral electron fluence error.	15
Figure 24.	Sun-Synchronous orbit at 500 km integral proton fluence error.....	15
Figure 25.	Sun-Synchronous orbit at 500 km total dose error.	16
Figure 26.	Sun-Synchronous orbit at 750 km integral electron fluence error.	16
Figure 27.	Sun-Synchronous orbit at 750 km integral proton fluence error.....	17
Figure 28.	Sun-Synchronous orbit at 750 km total dose error.	17
Figure 29.	Sun-Synchronous orbit at 1500 km integral electron fluence error.	18
Figure 30.	Sun-Synchronous orbit at 1500 km integral proton fluence error.....	18
Figure 31.	Sun-Synchronous orbit at 1500 km total dose error.	19
Figure 32.	Mid-Inclined LEO at 400 km integral electron fluence error.	19
Figure 33.	Mid-Inclined LEO at 400 km integral proton fluence error.....	20
Figure 34.	Mid-Inclined LEO at 400 km total dose error.....	20

Tables

Table 1.	Orbital Parameters of Mission Orbits Used in the Validation Study	4
----------	---	---

1. Introduction

The AE9/AP9 radiation environment models are an update to the NASA AE8/AP8 models. Unlike AE8/AP8, which were a set of static 3D lookup tables, AE9/AP9 provides more information in the form of statistics that account for solar cycle variability and systematic measurement uncertainties [1]. As such, AE9/AP9 procedurally generates its environmental data based on the user inputs every time it is run. Depending on the user inputs, this method of producing data can sometimes take hours or days for a single run. In a conceptual design environment, it becomes necessary to reduce the turnaround time for analyses from hours or days down to seconds or minutes. Thus it would be advantageous to have a lookup table similar to AE8/AP8 that consists of AE9/AP9 data.

For this study, only the mean environment mode was used. AE9/AP9 model version 1.20.001 was used, but its methods should be applicable to all versions of the AE9/AP9 model.

2. Method

The AE9/AP9 model software allows the user to specify a spacecraft mission's orbital parameters and duration. The software will then use a propagator to produce a trajectory file consisting of one time dimension and three spatial dimensions per data point, readable by the AE9/AP9 software. The software can also read a customized trajectory file that has been produced outside of the AE9/AP9 propagator. It is the customized trajectory file that can be used to generate a 3D mesh similar to the AE8/AP8 lookup tables. Instead of passing a spacecraft orbit to the AE9/AP9 software, a trajectory file consisting of a series of points, all at the exact same time, and systematically varying in the three spatial dimensions to cover all of the near-Earth space in a grid could be passed to the AE9/AP9 software. The output would then be a snapshot of the radiation environment predicted by the AE9/AP9 model for all of space encapsulated by the input grid. Using this ability of the AE9/AP9 software, it is possible to generate large amounts of data that describe the near-Earth radiation environment.

Initial investigation of this method produced positive results. An arbitrary 3D grid was generated and passed through the AE9/AP9 model. The resulting output was used to construct a 3D data table that could be read by the Satellite Orbit Analysis Program (SOAP) [2], which is a program developed and maintained by The Aerospace Corporation. SOAP allows for a visualization of the 3D data table in 2D slices, as shown in Figure 1, and also allows for analysis of spacecraft orbits within the space encapsulated by a data table. Using SOAP, the same analysis could be performed that would be performed using the AE9/AP9 software, except using the data table in place of procedurally generating the particle flux data.

Early investigation into the agreeability of the 3D lookup table and the AE9/AP9 model for the same orbit was promising, but several issues were identified. The two main issues stemmed from the temporal nature of AE9/AP9 and the static nature of the lookup tables. The AE9/AP9 mean mode varies temporally with two fundamental frequencies, the Earth's rotation and the Earth's orbit around the sun. The other modes, can vary statistically to include other factors, such as solar activity and solar cycle.

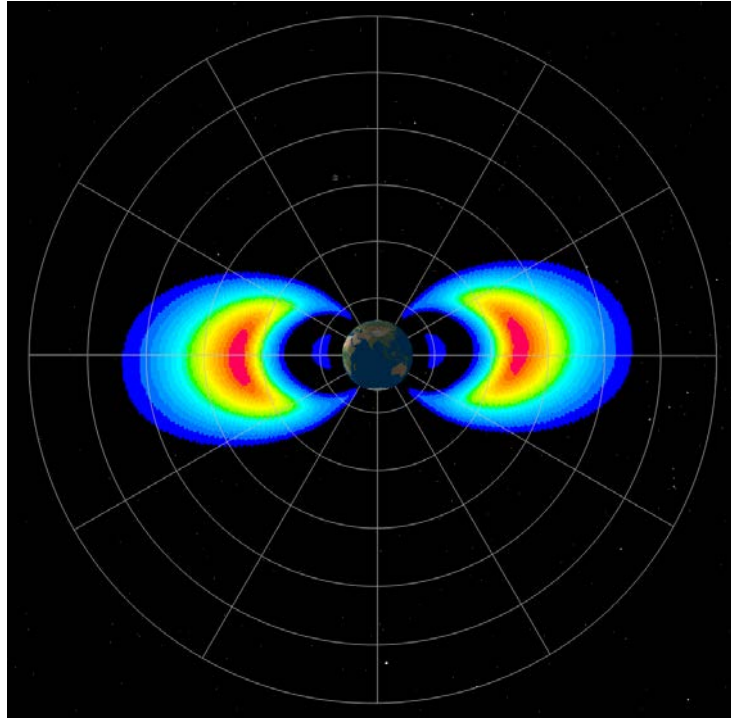


Figure 1. Visualization of AE9 integral 1 MeV electrons using SOAP and a static 3D table containing data generated from the AE9/AP9 model.

The first temporal variation is on short time scales (hours) and is a function of the rotation of the Earth. This rotation of the Earth's magnetic field interacting with the solar wind produces some features that are highly dependent on the location of the sun in reference to the location within the magnetic field. The geomagnetic tail, for instance, is always pointed away from the sun along the Earth-sun vector. In a static 3D table, the geomagnetic tail will rotate with the Earth, meaning that there are times when the geomagnetic tail will be pointed toward the sun and other times when it will be pointed 90 deg to the Earth-sun vector, instead of always being pointed anti-sun.

The second temporal variation is the result of the varying difference between the Earth's geomagnetic axis and the ecliptic plane. As the Earth moves from one solstice to the next, the geomagnetic tail changes latitude as the Earth's geomagnetic axis changes angle with the plane of the ecliptic. As such, the structure of the outer portion of the radiation belts will change throughout a year as the Earth moves through its orbit.

The first variation, which is a result of the rotation of the Earth, can be averaged out by generating a 4D data table and then averaging over the time dimension. To do this, a time step of one hour was chosen and the same spatial grid was run for 24 time steps. After all of the data had been generated, the time dimension is averaged out, resulting in a single 3D data table for the date selected.

The second variation, which was the result of the varying latitude of the geomagnetic tail as the Earth orbited around the sun, can be averaged out by generating several 3D tables on different days of the year, using the method outlined in the previous paragraph, and then averaging over the different days. To do this, the spring and fall equinoxes as well as the summer and winter solstices were selected based on the U.S. Naval Observatory website [3]. 3D data tables were generated for each of these days and the final 3D data tables were a result of averaging over these four days.

Using these methods of accounting for the temporal variations means that, while the results between the static lookup tables and the dynamic AE9/AP9 model will agree for mission orbits lasting years; on a time scale shorter than a year there may be some disagreement. The impact of short time scales on the agreeability was not looked into due to the focus on long-term mission orbits in this study.

The 3D grid itself was also a cause for disagreement between the initial lookup tables and the AE9/AP9 model. A large number of data points are desirable because that would minimize the pixilation error in the data tables. As the number of data points increases, however, the physical size of the data tables, the amount of computer time needed to initially produce the tables, and the amount of time needed to load the tables into memory for analysis, increases. A low fidelity is undesirable, but if the data tables are too large, they can be difficult to produce in a timely manner without a large number of available computer cores, and once they are produced, if the data tables are too large it can take a large amount of time to read them into memory for analysis.

The initial grid consisted of a geodetic set of altitudes, latitudes, and longitudes. The altitudes went from 0 km to 50,000 km in steps of 200 km, the latitudes went from 0 deg to 360 deg in steps of 5 deg, and the longitudes went from -90 deg to 90 deg in steps of 2 deg. This produced a data grid that encompassed all of the near-Earth space in a sphere that extends well beyond the geosynchronous altitude. A validation study showed that the LEO orbits had larger than desired disagreement with the AE9/AP9 model, while the higher altitude orbits agreed fairly well. It was determined that the altitude steps of 200 km were too large for the LEO region, where the radiation environment changes quickly with altitude.

To alleviate this issue, a variable altitude step was introduced into the data tables. An altitude step of 20 km was used from 0 to 1,500 km, an altitude step of 50 km was used from 1,550 to 5,000 km, and an altitude step of 200 was used beyond 5,200 km. An altitude step of 10 km was used from 35,610 to 36,000 to encapsulate the geosynchronous region.

It was also found that latitudes at -86 deg and below, as well as 78 deg and above, contained no flux data output from the AE9/AP9 model, so these latitudes were removed from the grid. Additional post-processing removed additional altitudes and latitudes where no flux data existed at each energy level in order to minimize the data table size.

Each particle energy level for flux, as well as each shield thickness for dose rate, was broken out into a separate data table.

3. Validation Study

To assess the agreeability between the AE9/AP9 model software output and the static 3D table analysis outputs, a series of mission orbits were run through the AE9/AP9 model and also through the static 3D tables using SOAP. A calculation of the percent error was made using:

$$\%Error = \frac{3D\ Table\ Output - AE9AP9\ Output}{AE9AP9\ Output} * 100 \quad \text{Eq. 1}$$

Using this equation, an error of close to zero means that the 3D table output was equal to the AE9/AP9 output, a positive error means that the 3D table output was overestimating the environment, and a negative error meant that the 3D table output was underestimating the environment. In the discussions in the following sections, the error will be referred to in absolute terms.

The AE9/AP9 propagation software was used to generate a trajectory file for the model to ingest, and SOAP used its own propagation algorithms. Both methods used the same inputs as listed in Table 1 for a variety of different orbits. The resulting parameters compared for all orbits were the integral particle fluence of electrons and protons at all energy levels as well as the final dose behind a range of shield thicknesses at the end of exactly one year in the mission orbit (January 1, 2015 00:00:00 through January 1, 2016 00:00:00). The proton and electron energy levels are the defaults from the AE9/AP9 v1.20.001 GUI. If an energy level produced no fluence data, or if the AE9/AP9 models output a fluence but the static tables did not, they were excluded from the graphs. The total dose assumed an aluminum shield and silicon detector with a spherical geometry with shielding thicknesses ranging from 15 to 800 mils.

Table 1. Orbital Parameters of Mission Orbits Used in the Validation Study

Orbit Type	Semi-Major Axis (km)	Argument of Perigee (deg)	RAAN (deg)	Eccentricity	Inclination (deg)
GEO	42166.35	0	0	0	0
GIO	42166.35	0	0	0	20
Tundra Orbit	42166.35	270	0	0.2684	63.4
Magic Orbit	10560.01	270	0	0.3467	116.6
Molniya Orbit	26551.84	270	0	0.725	63.435
PNT Orbit	26551.84	0	0	0	55
Sun Synchronous at 350 km	6728.134	0	0	0	96.854
Sun Synchronous at 500 km	6878.134	0	0	0	97.4
Sun Synchronous at 750 km	7128.134	0	0	0	98.4
Sun Synchronous at 1500 km	7878.134	0	0	0	101.96
Mid Inclined LEO at 400 km	6780	0	0	0	51.64

3.1 GEO Results

The geostationary orbit (GEO) is a circular orbit with a one-day orbit period and zero inclination. The static tables and the AE9/AP9 models show good agreement. For electrons above 6 MeV, the error is greater than 5%. For protons, the error is less than 5%, except for at 4 MeV, where the error is at 25%. The total dose error is contained below 3.5% for the full range of shield thicknesses. Figure 2, Figure 3, and Figure 4 show the error between the static tables and the AE9/AP9 models for electron fluence, proton fluence, and total dose, respectively, for this geostationary orbit.

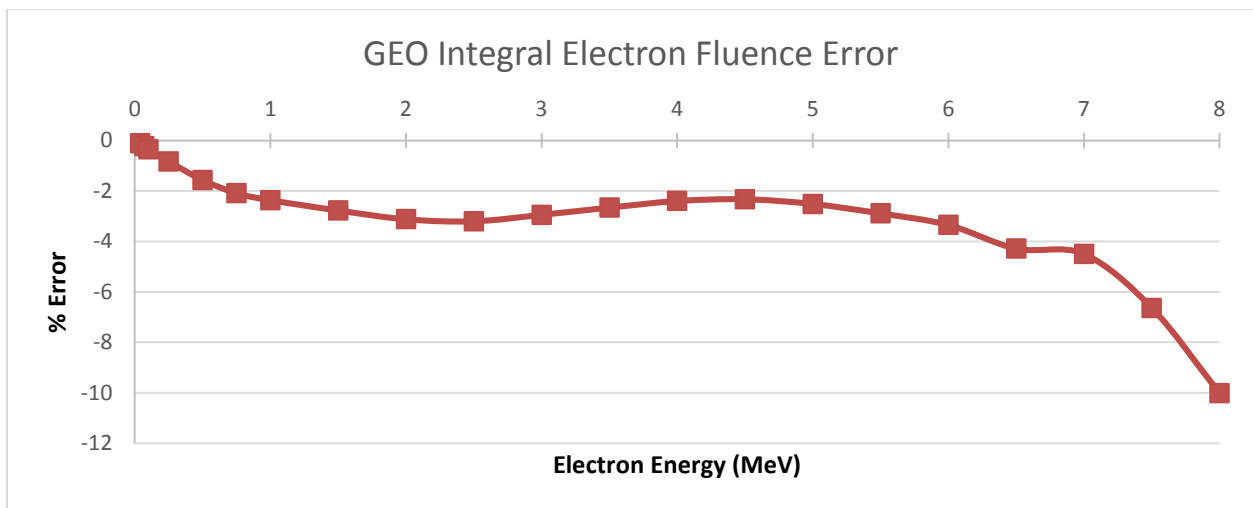


Figure 2. GEO integral electron fluence error.

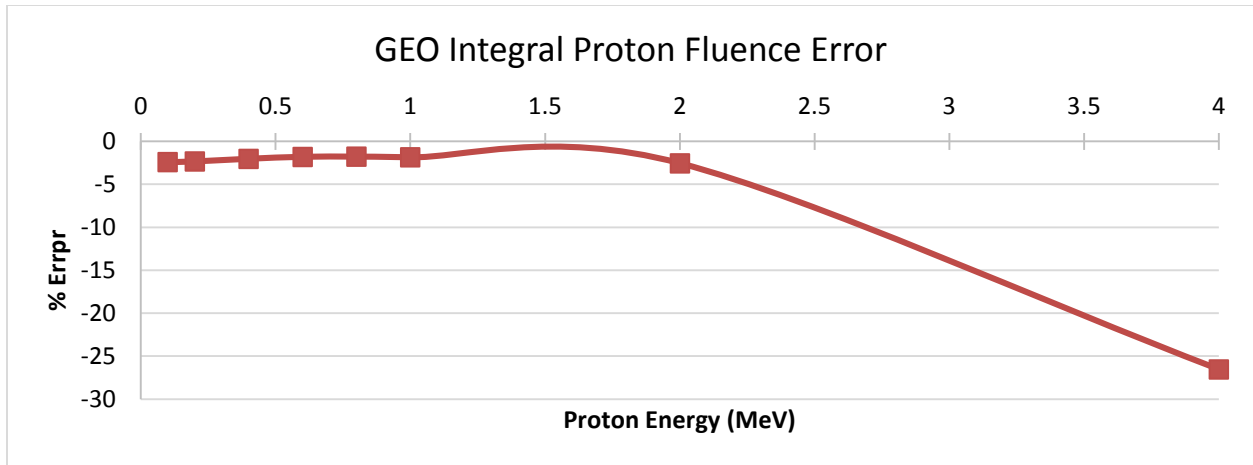


Figure 3. GEO integral proton fluence error.

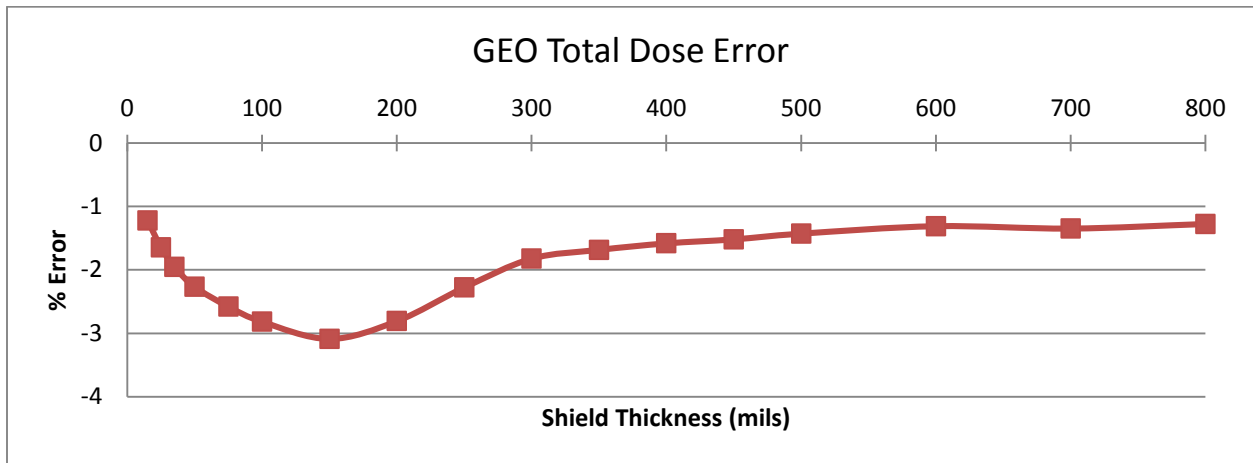


Figure 4. GEO total dose error.

3.2 GIO Results

The geosynchronous-inclined (GIO) orbit is similar to the geostationary orbit, but with an inclination of 20 deg. In this orbit, the electrons, protons, and dose all show good agreement between the static tables and the AE9/AP9 models. The electrons have an error less than 5% below 6.5 MeV, and less than 10% at all energy levels. The protons have an error between 0% and 3%. The total dose error less than 2.5% for the full range of shield thicknesses. Figure 5, Figure 6, and Figure 7 show the error between the static tables and the AE9/AP9 models for electron fluence, proton fluence, and total dose, respectively, for this geosynchronous-inclined orbit.

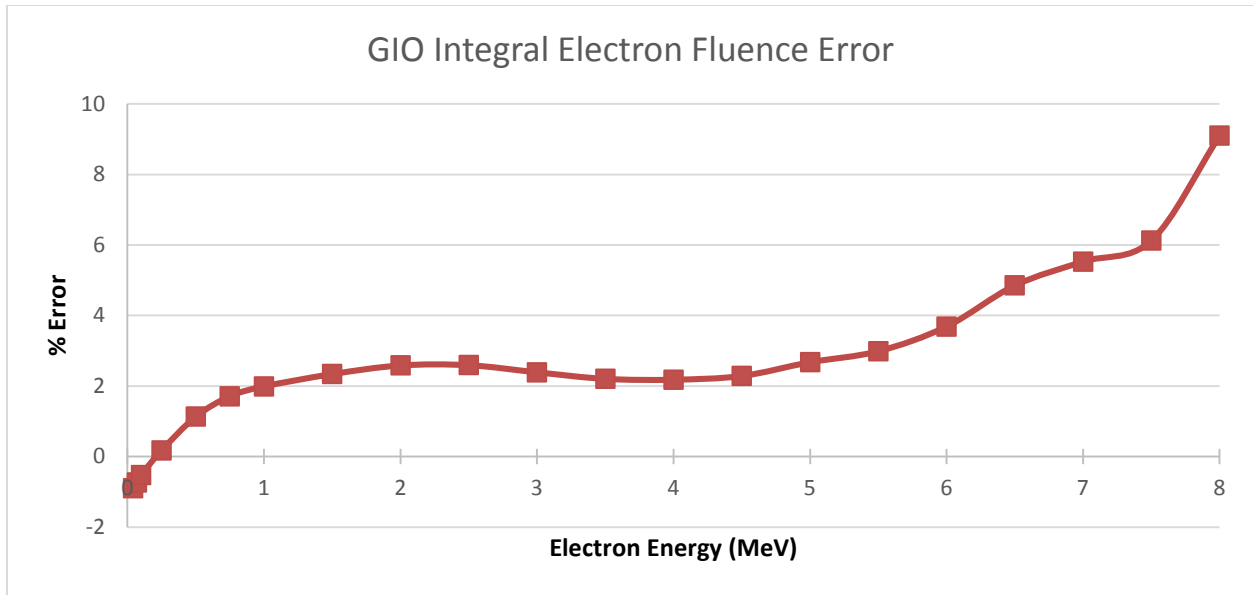


Figure 5. GIO integral electron fluence error.

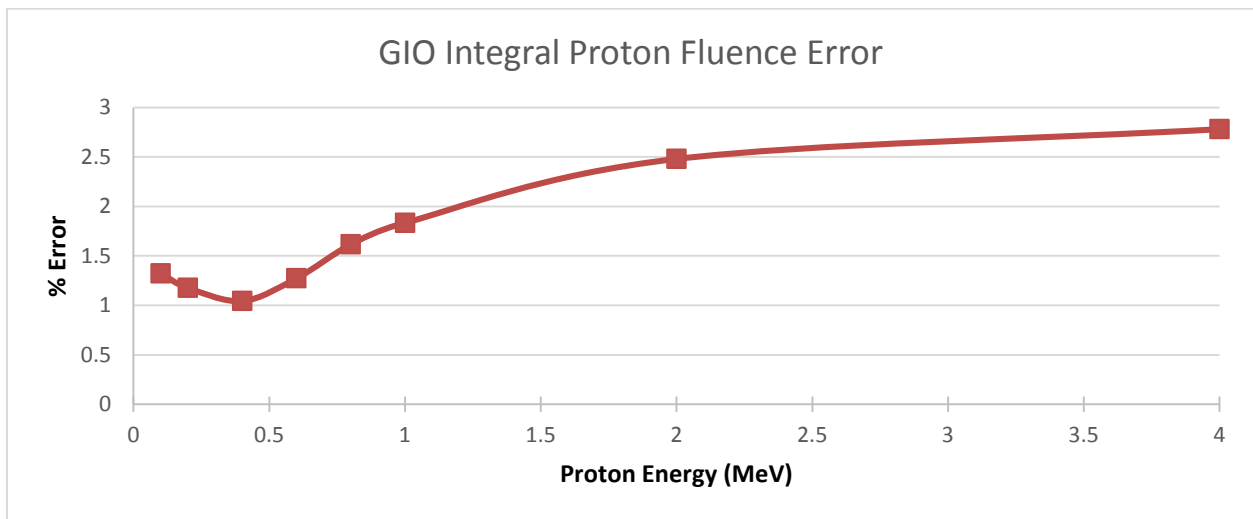


Figure 6. GIO integral proton fluence error.

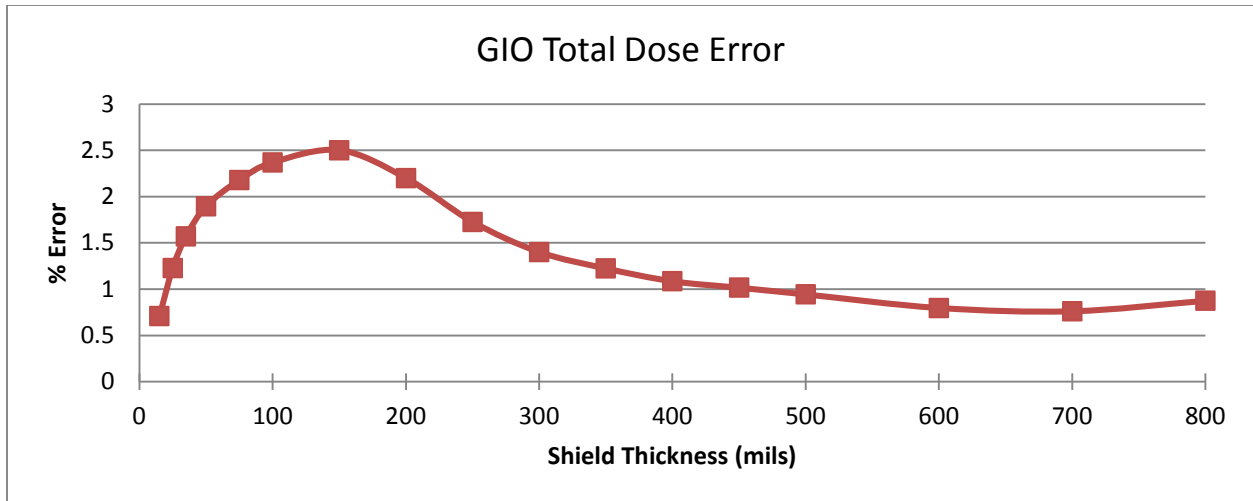


Figure 7. GIO total dose error.

3.3 Tundra Orbit Results

The Tundra orbit is an orbit with a period of one day and is slightly elliptical and critically inclined. In this orbit, the agreement between the static tables and the AE9/AP9 models is very good, with the electron error less than 3%, proton error between 1.5% and 2%, and total dose error less than 2.5%. Figure 8, Figure 9, and Figure 10 show the error between the static tables and the AE9/AP9 models for electron fluence, proton fluence, and total dose, respectively, for this Tundra orbit.

Not shown in Figure 9 is the case for protons at 6 MeV. In this case, the AP9 model reported a low fluence count while the static tables reported nothing, resulting in a 100% error. The integral fluence at 4 MeV was 2×10^7 particles/cm², while the integral fluence at 6 MeV was 5×10^3 particles/cm², representing a steep drop-off in the particle environment between these two energy levels.

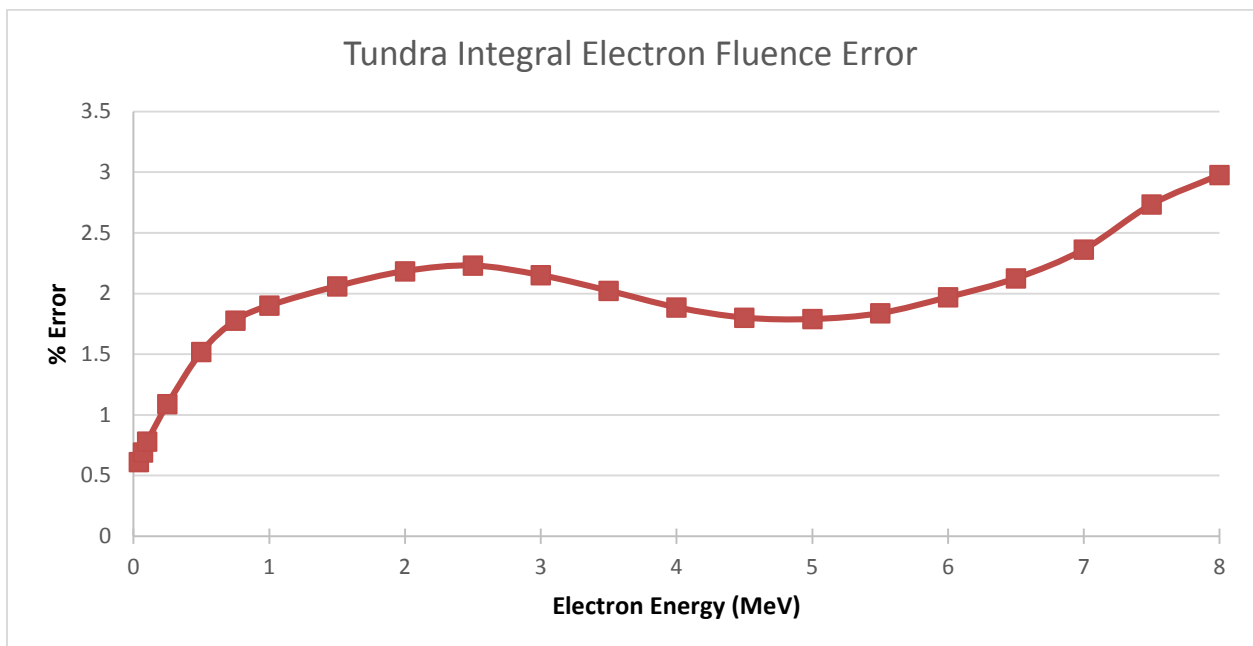


Figure 8. Tundra orbit integral electron fluence error.

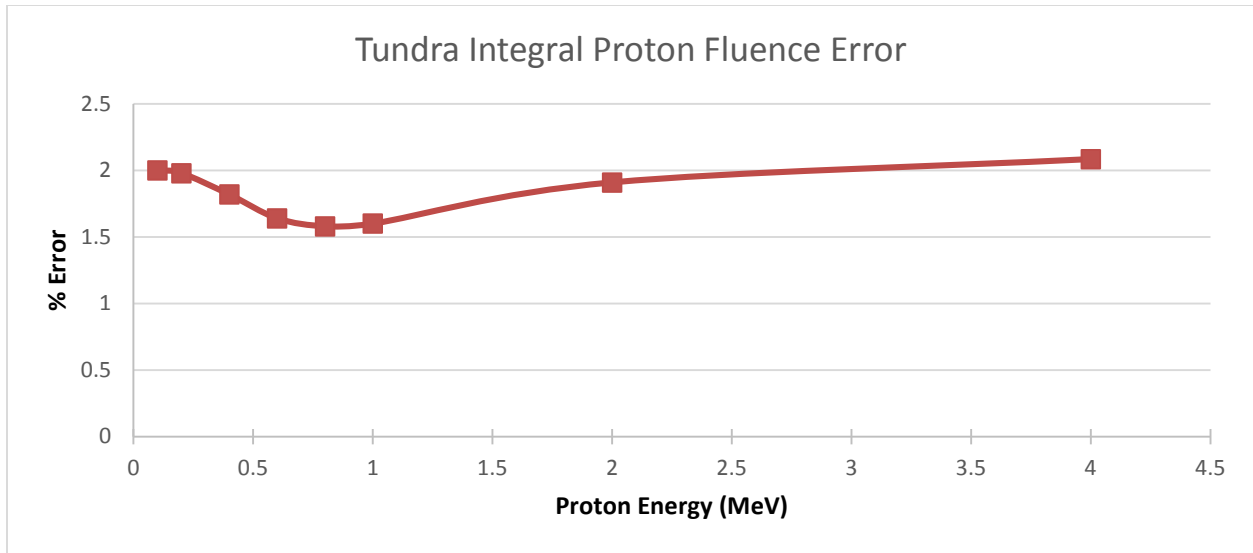


Figure 9. Tundra orbit integral proton fluence error.

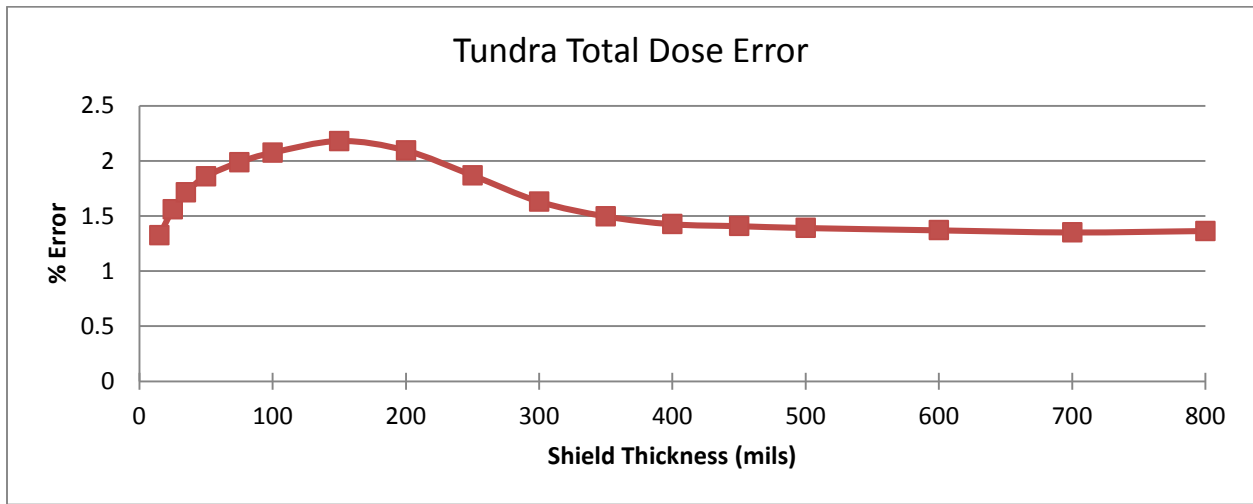


Figure 10. Tundra orbit total dose error.

3.4 Magic Orbit Results

The magic orbit is a critically inclined orbit with a three-hour period and a repeating ground track. The agreement between the static tables and the AE9/AP9 models is very good for all particles and energy levels. For electrons, the general error is below 3%, except for the 7.5 and 8 MeV cases, where the error is 3.6% and 7.2%, respectively. For protons, the error is below 1% for all cases except at 0.1 MeV, where the error is 1.1%. For total dose, the error is below 1.2% for all shield thicknesses. Figure 11, Figure 12, and Figure 13 show the error between the static tables and the AE9/AP9 models for electron fluence, proton fluence, and total dose, respectively, for this magic orbit.

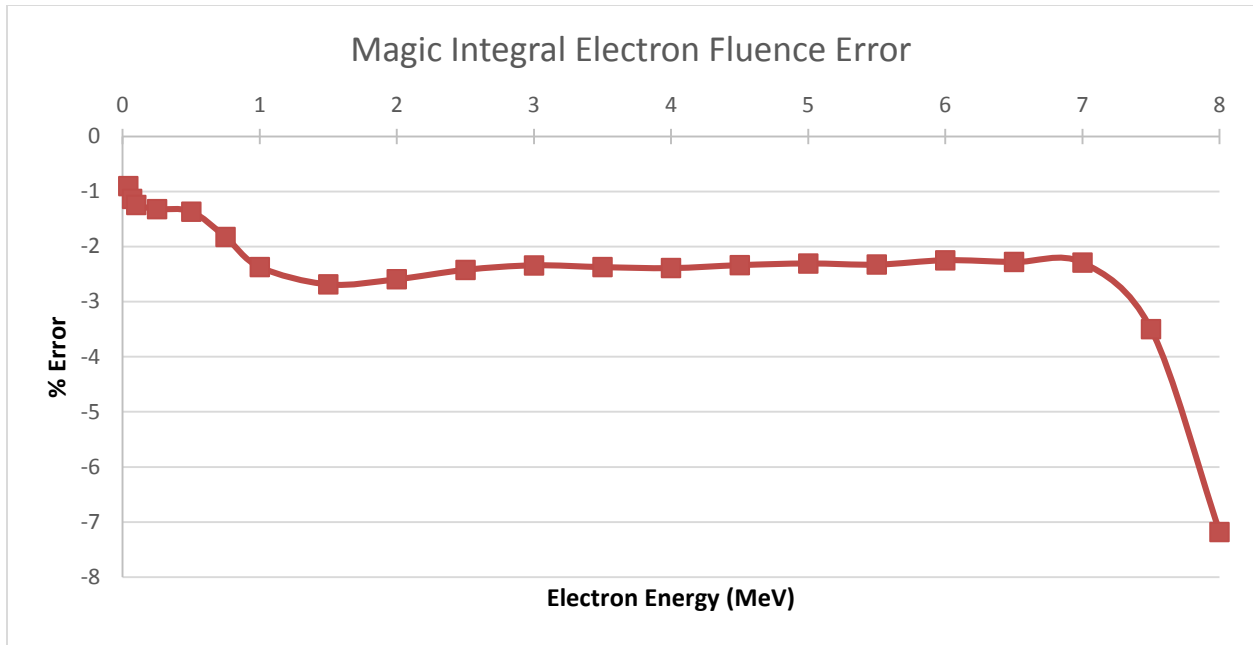


Figure 11. Magic orbit integral electron fluence error.

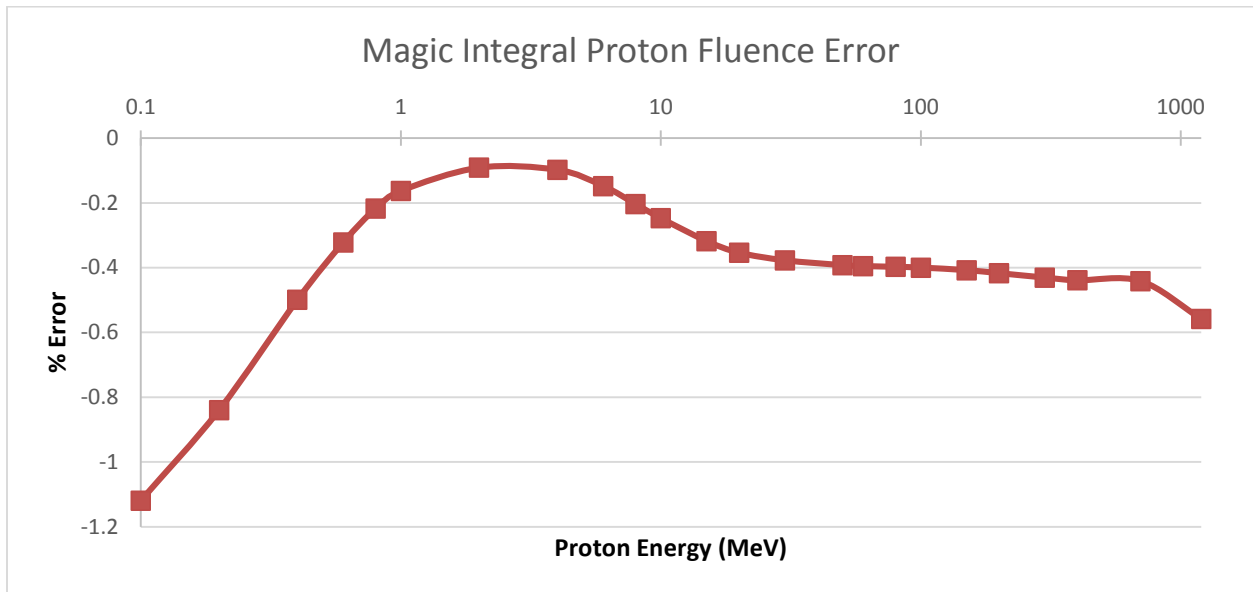


Figure 12. Magic orbit integral proton fluence error.

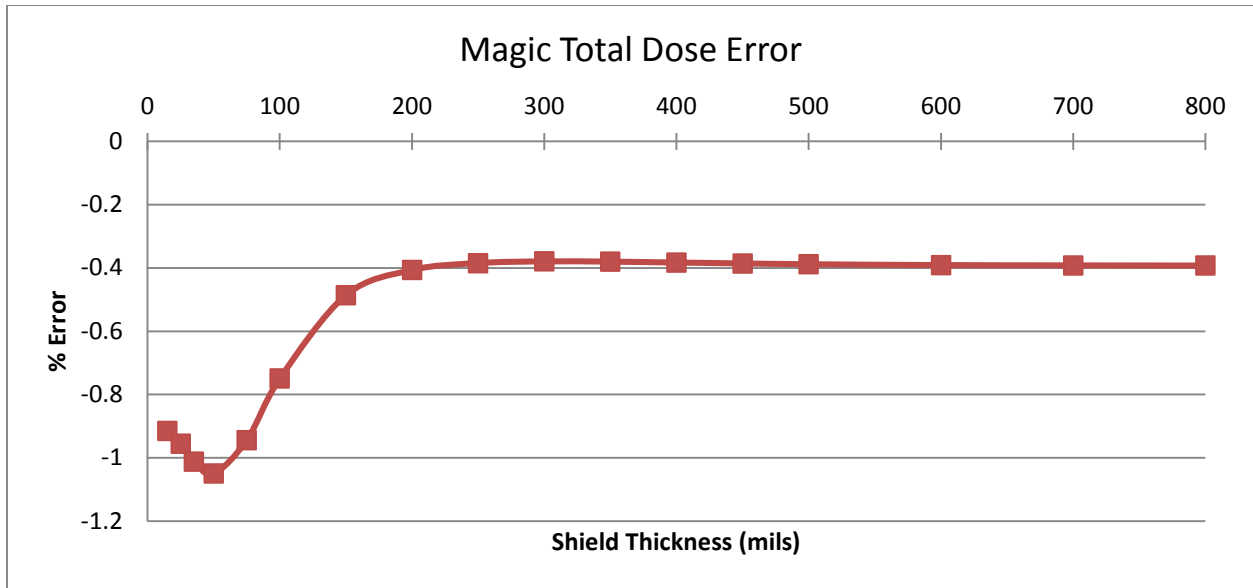


Figure 13. Magic orbit total dose error.

3.5 Molniya Orbit Results

The Molniya orbit is a highly elliptical, critically inclined orbit. The static tables and the AE9/AP9 models show very good agreement at all electron and proton energy levels. The electron error is below 1% at energies at all energies except at 8 MeV, where it is 1.04%. The proton error is at or below 3.5% below 200 MeV and grows to 5-6% at 700 to 1200 MeV. For total dose, the error is low at low shielding thicknesses and grows to 3.25% error above 300 mils. Figure 14, Figure 15, and Figure 16 show the error between the static tables and the AE9/AP9 models for electron fluence, proton fluence, and total dose, respectively, for this Molniya orbit.

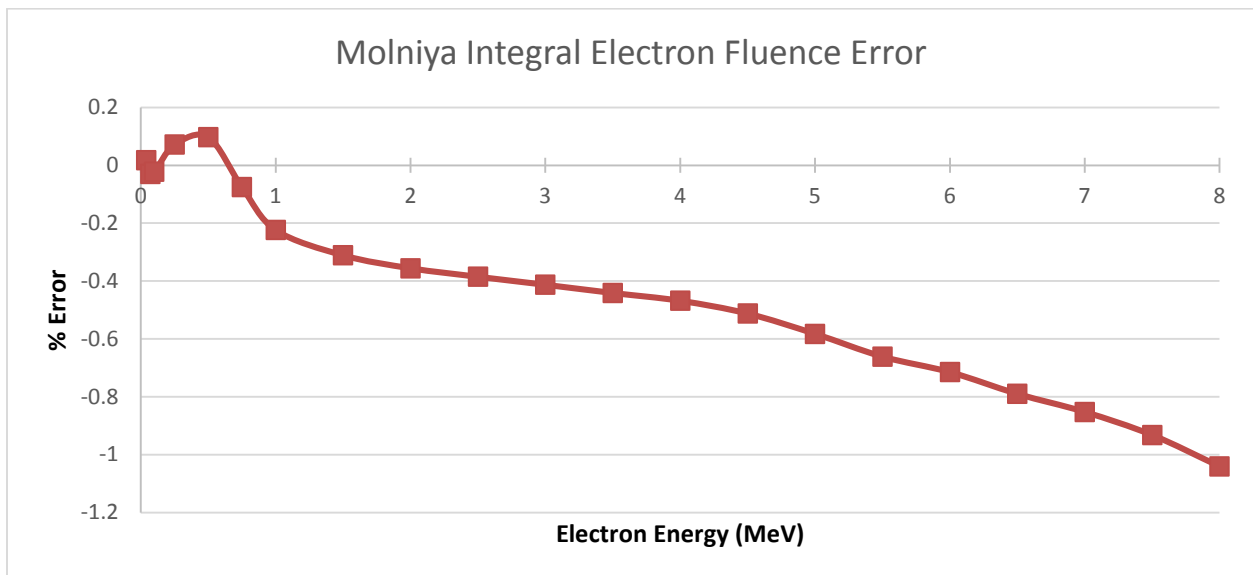


Figure 14. Molniya orbit integral electron fluence error.

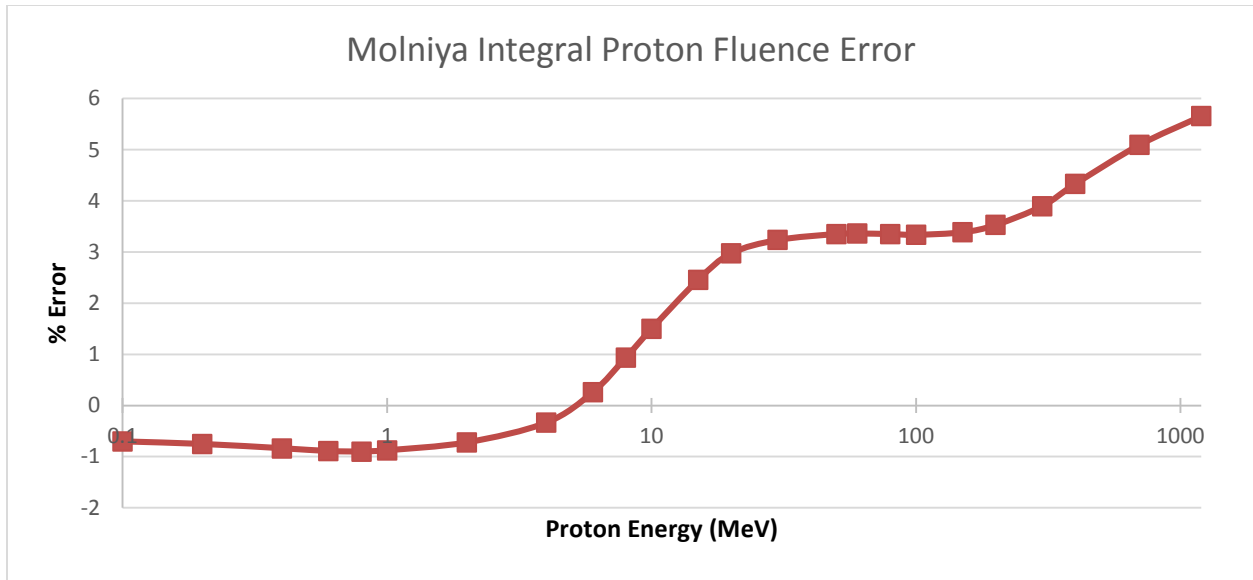


Figure 15. Molniya orbit integral proton fluence error.

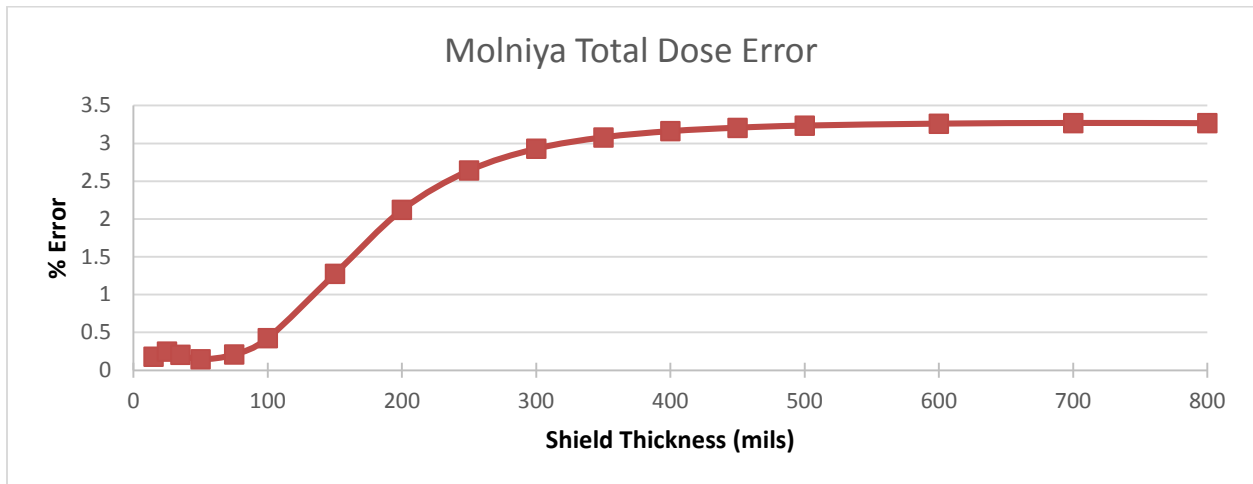


Figure 16. Molniya orbit total dose error.

3.6 PNT Orbit Results

The Position, Navigation, and Timing (PNT) orbit is a circular orbit with a half-day orbit period and a 55-deg inclination. There is very good agreement between the static tables and the AE9/AP9 models. The electrons have an error less than 0.6% at all energy levels, the protons have an error less than 1.1% at all energy levels shown, and the total dose error is less than 0.2% at all shielding thicknesses. Figure 17, Figure 18, and Figure 19 show the error between the static tables and the AE9/AP9 models for electron fluence, proton fluence, and total dose, respectively, for this PNT orbit.

Not shown in Figure 18 are the cases for protons at 8, 10, and 15 MeV. In these cases, the AP9 model reports a fluence count while, with the exception of the 8 MeV case, the static tables do not. For the 8 MeV case, the static tables report a fluence of $1e5$ particles/cm², while the AP9 model reports a fluence of $1e6$ particles/cm². For the 10 and 15 MeV cases, the static tables report no fluence while the AP9 model does, though they are very low fluences compared to the slightly lower energy levels. For instance, the AP9 model reports a fluence of 541 particles/cm² for the 15 MeV case.

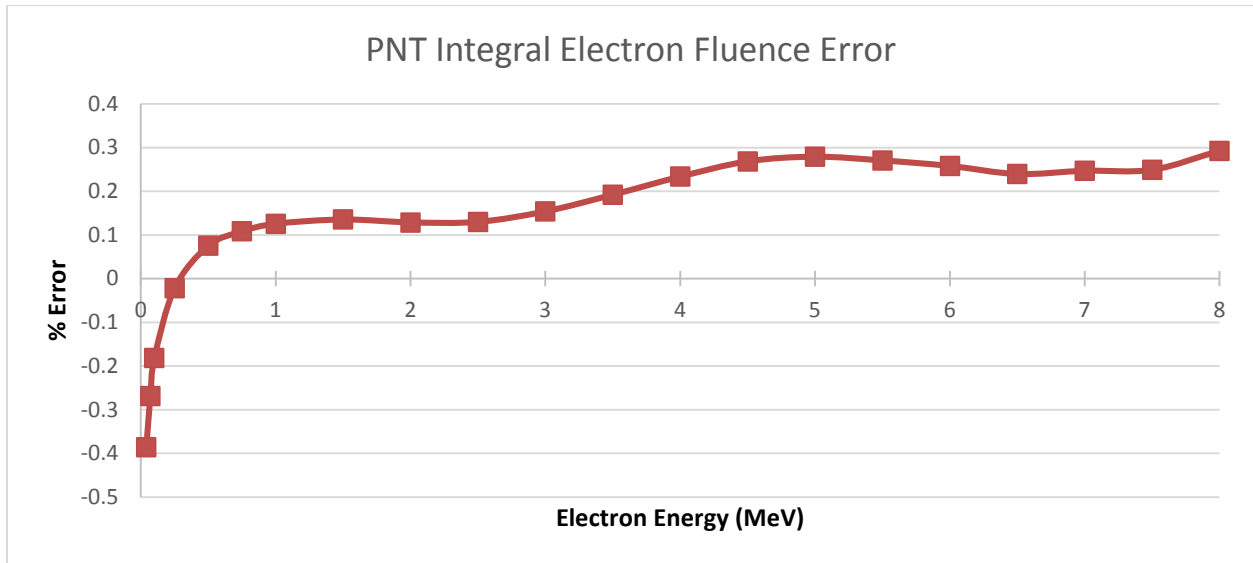


Figure 17. PNT orbit integral electron fluence error.

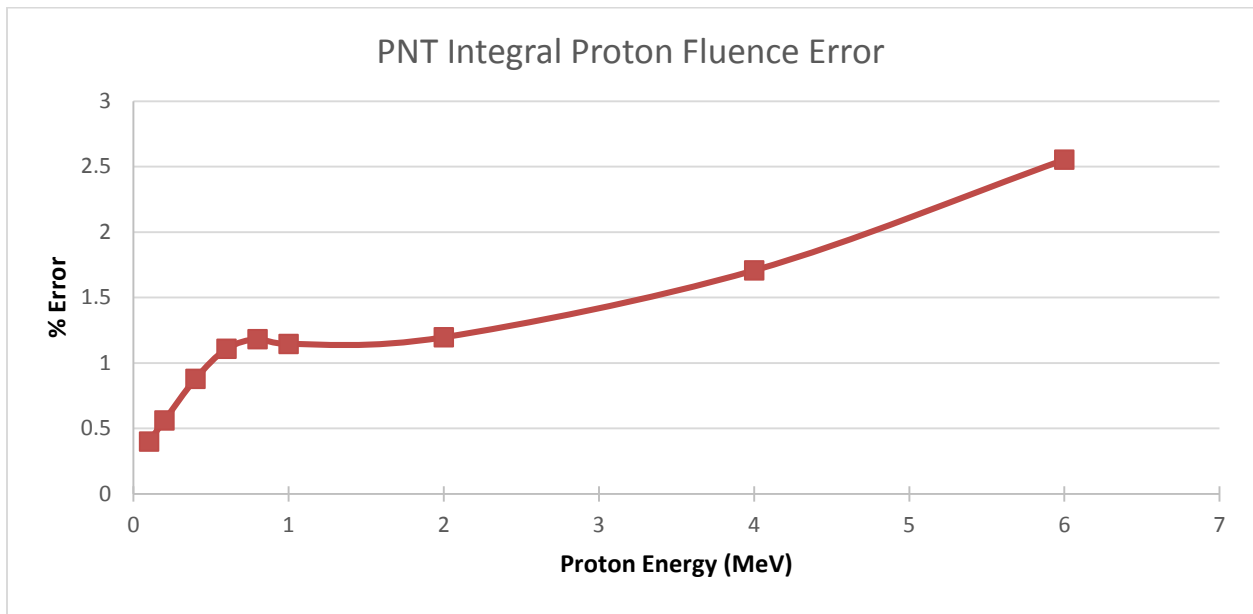


Figure 18. PNT orbit integral proton fluence error.

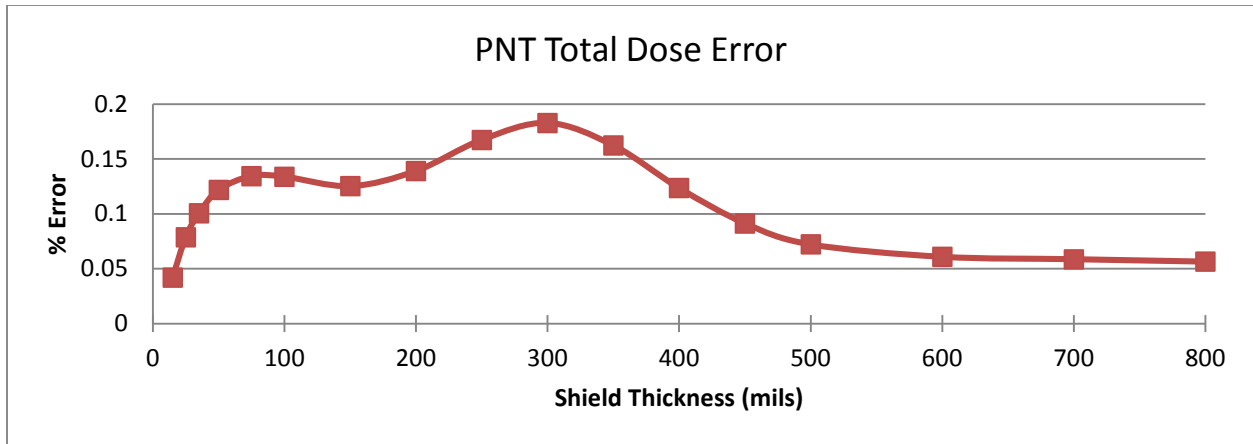


Figure 19. PNT orbit total dose error.

3.7 Sun Synchronous Orbit at 350 km Results

This sun synchronous orbit is a low-earth orbit (LEO) with an altitude of 350 km and an inclination of 96.9 deg. This orbit has good agreement between the static tables and the AE9/AP9 models. The electrons have an error of ~5% from the low energies up to 5 MeV, at 5.5 MeV the error increases to 10% and then 28% at 6 MeV. The protons have an error that is between 4% and 6% below 8 MeV, and shrinks to less than 3% as the energy level grows. The total dose error is fairly constant between 3% and 4.5% for all shield thicknesses. Figure 20, Figure 21, and Figure 22 show the error between the static tables and the AE9/AP9 models for electron fluence, proton fluence, and total dose for this sun synchronous orbit respectively.

Not shown in Figure 21 is the case for protons at 1200 MeV. In this case, the AP9 model reports a fluence count while the static tables do not, resulting in a 100% error. The fluence reported by the AP9 model for 700 MeV protons is $3e5$ while the fluence for 1200 MeV protons is 121 representing a steep drop off in the particle environment between these two energy levels.

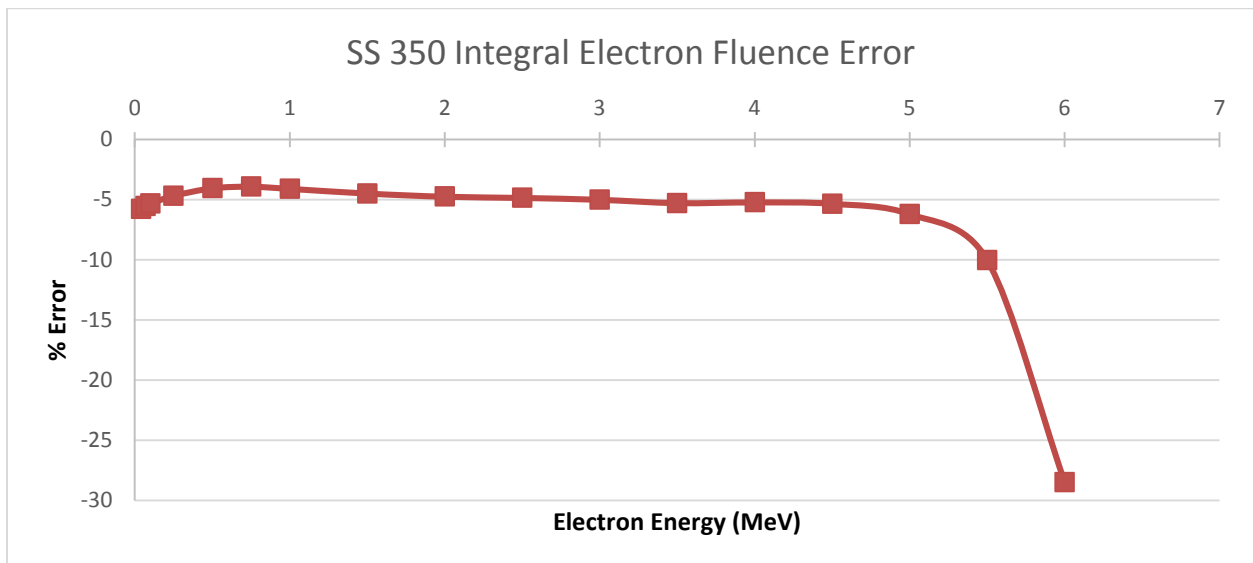


Figure 20. Sun-Synchronous orbit at 350 km integral electron fluence error.

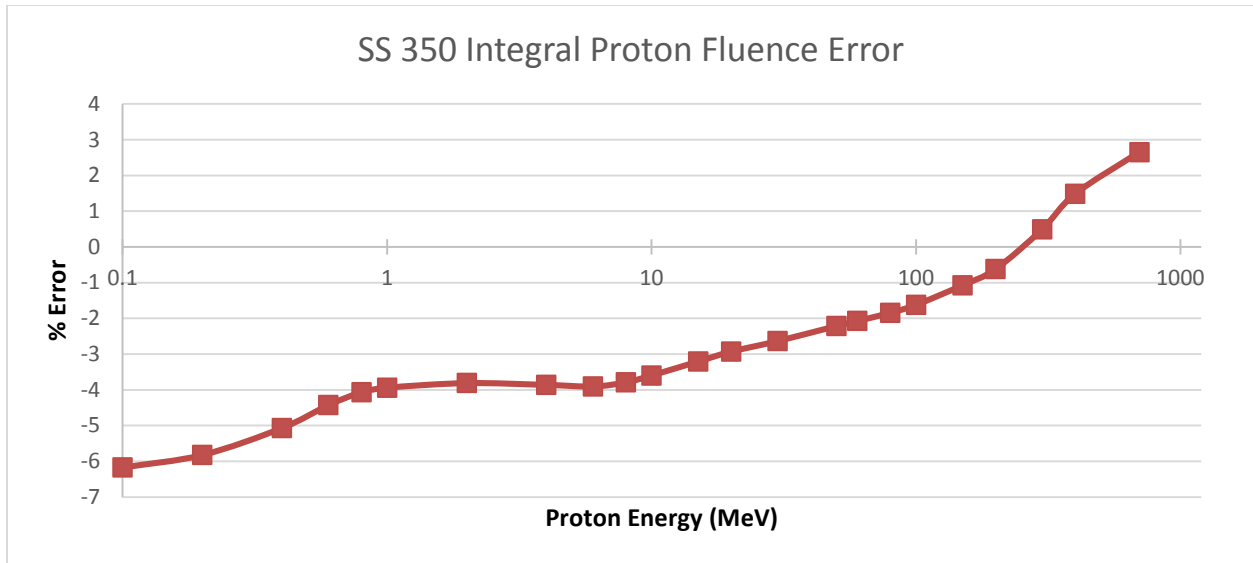


Figure 21. Sun-Synchronous orbit at 350 km integral proton fluence error.

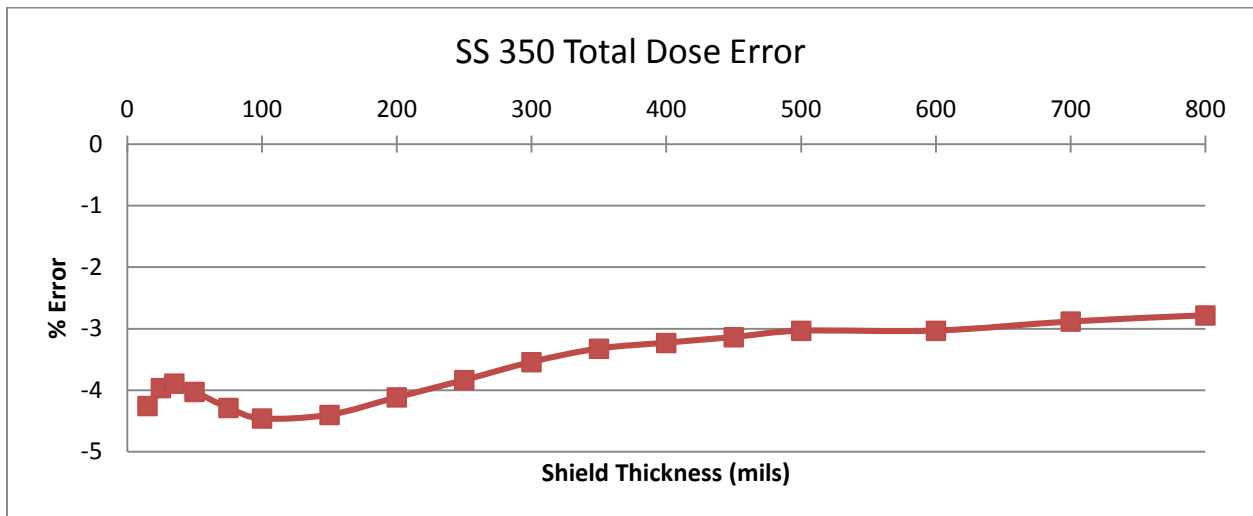


Figure 22. Sun-Synchronous orbit at 350 km total dose error.

3.8 Sun Synchronous Orbit at 500 km Results

This sun synchronous orbit is a LEO with an altitude of 500 km and an inclination of 97.4 deg. This orbit has good agreement between the static tables and the AE9/AP9 models. The electrons have an error between 2% and 6%. The protons have an error that starts at 6% but shrinks to ~0% as the energy level increases, however the error jumps to 10% at 1200 MeV. The total dose error is fairly consistent between 2.5% and 3% for all shield thicknesses. Figure 23, Figure 24, and Figure 25 show the error between the static tables and the AE9/AP9 models for electron fluence, proton fluence, and total dose for this sun synchronous orbit respectively.

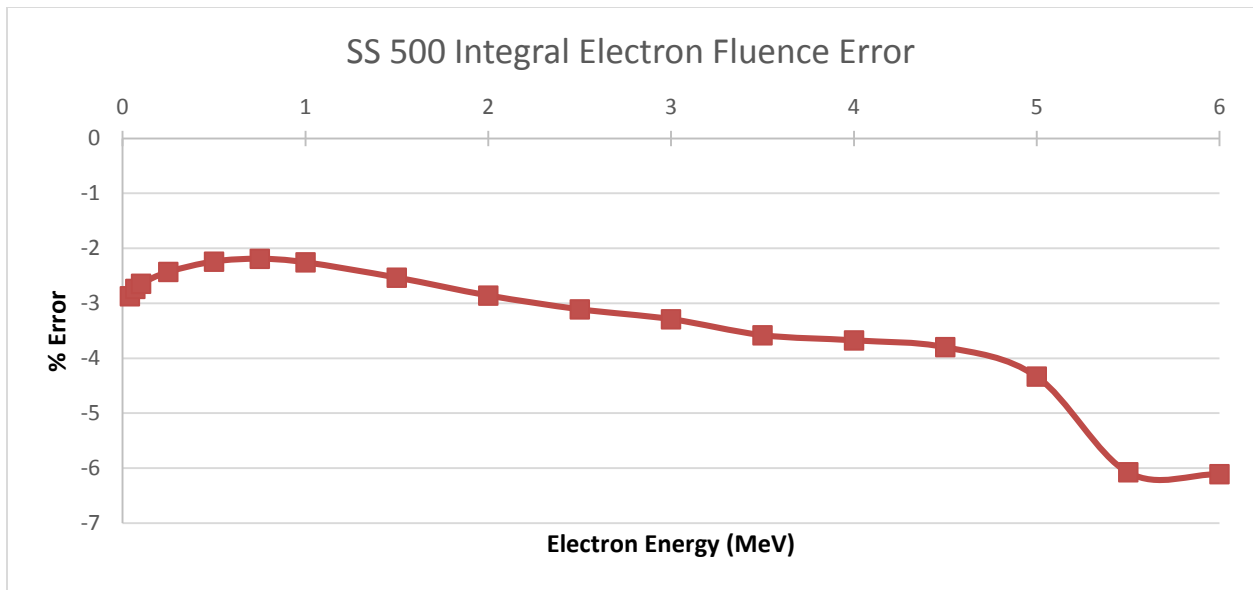


Figure 23. Sun-Synchronous orbit at 500 km integral electron fluence error.

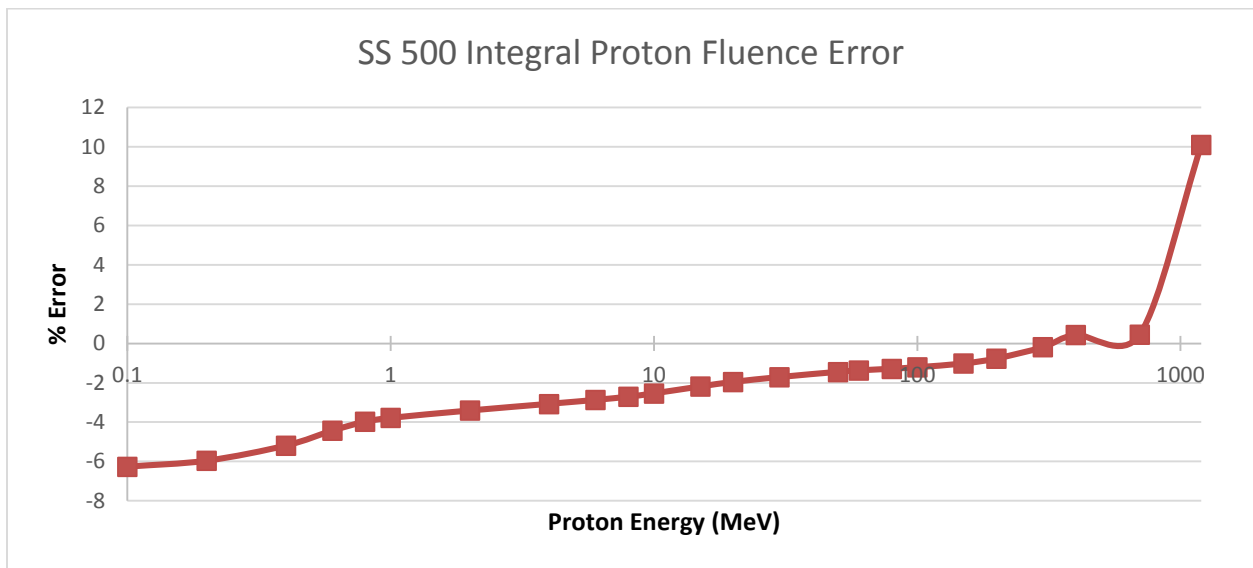


Figure 24. Sun-Synchronous orbit at 500 km integral proton fluence error.

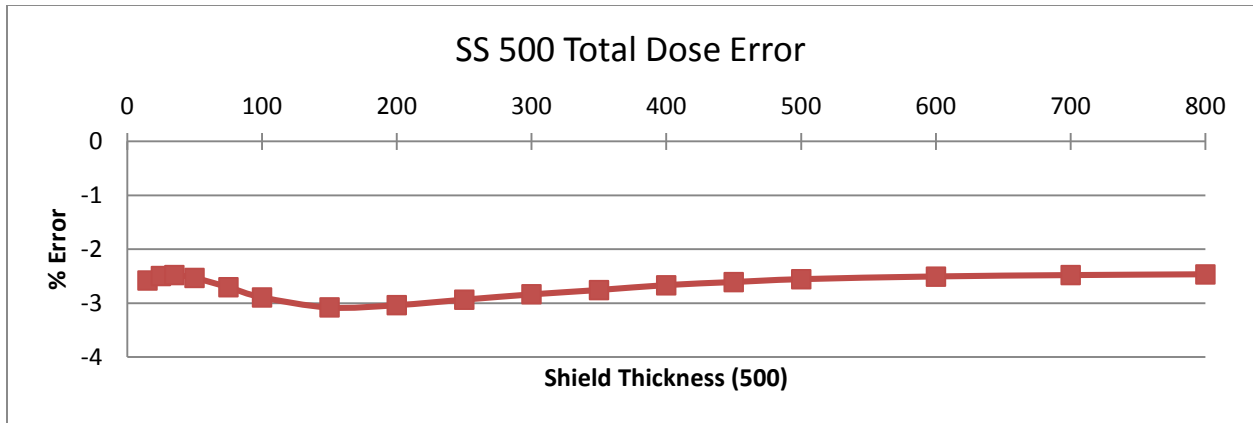


Figure 25. Sun-Synchronous orbit at 500 km total dose error.

3.9 Sun Synchronous Orbit at 750 km Results

This sun synchronous orbit is a LEO with an altitude of 750 km and an inclination of 98.4 deg. This orbit has very good agreement between the static tables and the AE9/AP9 models. The electrons have an error between 2.5% and 3% for most energy levels. The protons have an error that starts at 3.7% but shrinks to less than 1.5% as the energy level increases. The total dose error at low shielding thicknesses starts at 2.5% and shrinks to 0% above 300 mils. Figure 26, Figure 27, and Figure 28 show the error between the static tables and the AE9/AP9 models for electron fluence, proton fluence, and total dose for this sun synchronous orbit respectively.

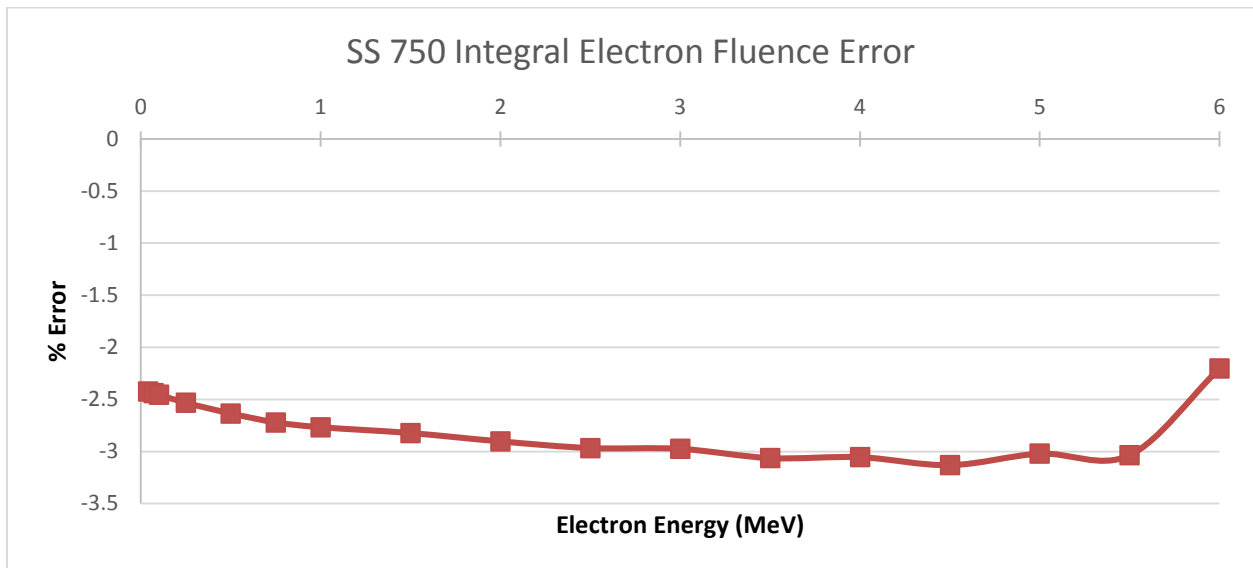


Figure 26. Sun-Synchronous orbit at 750 km integral electron fluence error.

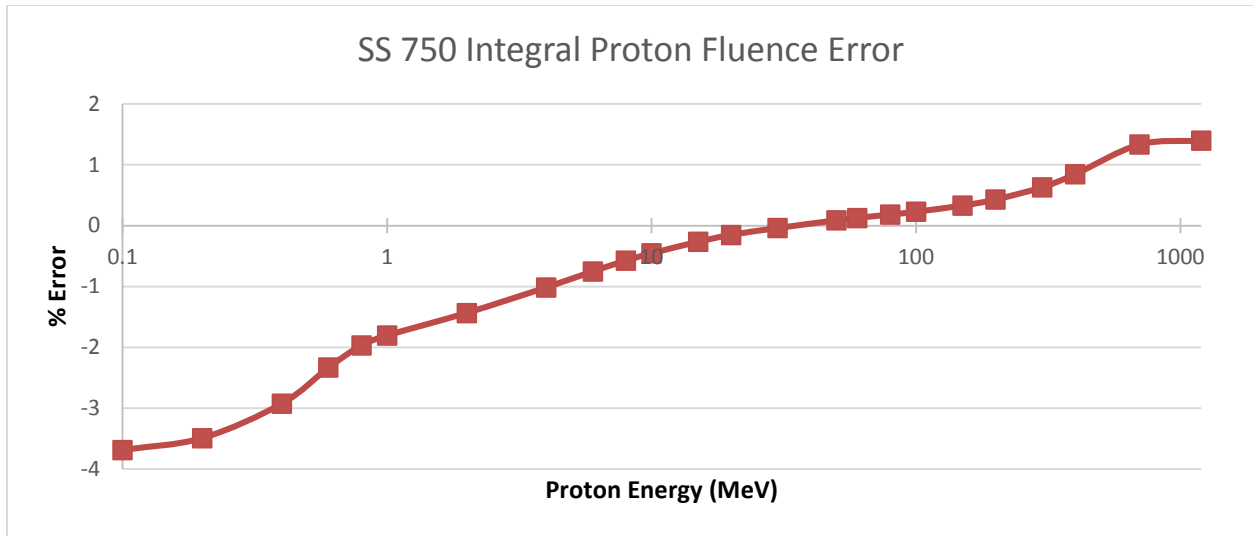


Figure 27. Sun-Synchronous orbit at 750 km integral proton fluence error.

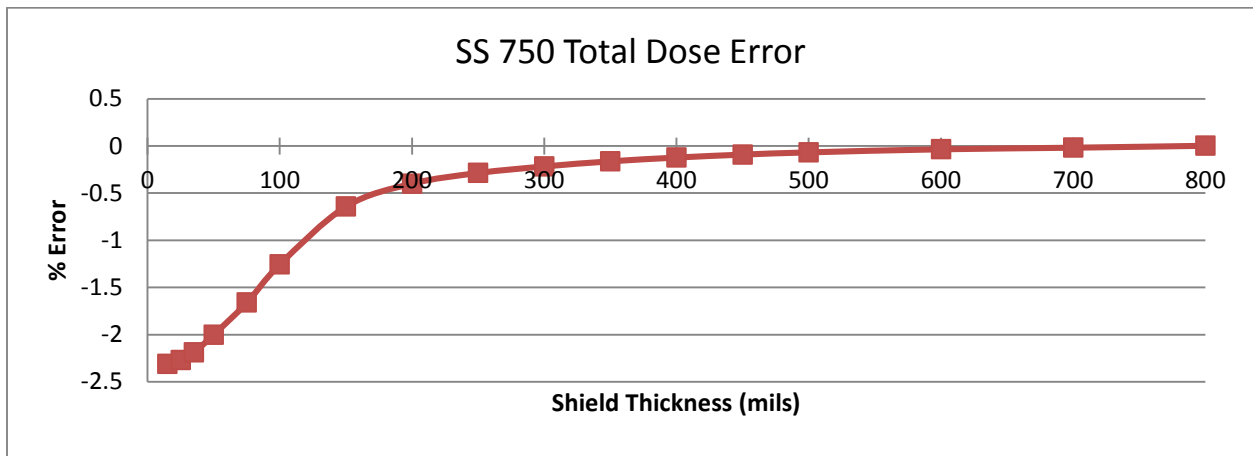


Figure 28. Sun-Synchronous orbit at 750 km total dose error.

3.10 Sun Synchronous Orbit at 1500 km Results

This sun synchronous orbit is a LEO with an altitude of 1500 km and an inclination of 116.6 deg. This orbit has very good agreement between the static tables and the AE9/AP9 models. The electrons have an error between 1% and 2% for all energy levels except for 6.5 MeV where it is 15%. The protons have an error that starts at 1.3% but shrinks to less than 0.5% at 4 MeV and above. The total dose error starts at 0.65% and drops to less than 0.3% above 150 mils. Figure 29, Figure 30, and Figure 31 show the error between the static tables and the AE9/AP9 models for electron fluence, proton fluence, and total dose for this sun synchronous orbit respectively.

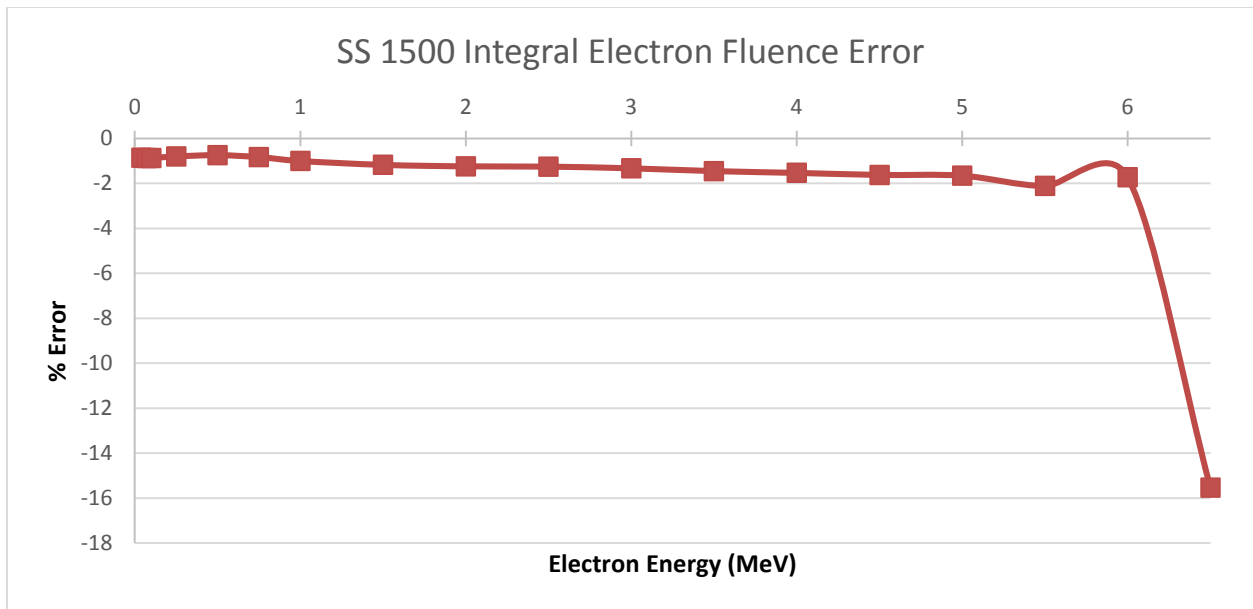


Figure 29. Sun-Synchronous orbit at 1500 km integral electron fluence error.

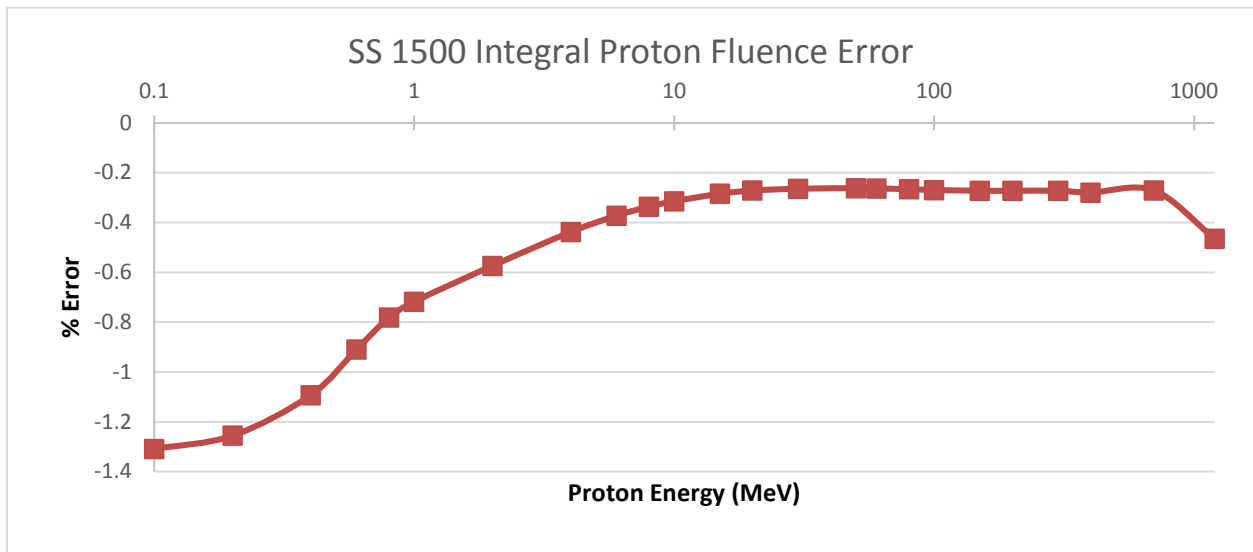


Figure 30. Sun-Synchronous orbit at 1500 km integral proton fluence error.

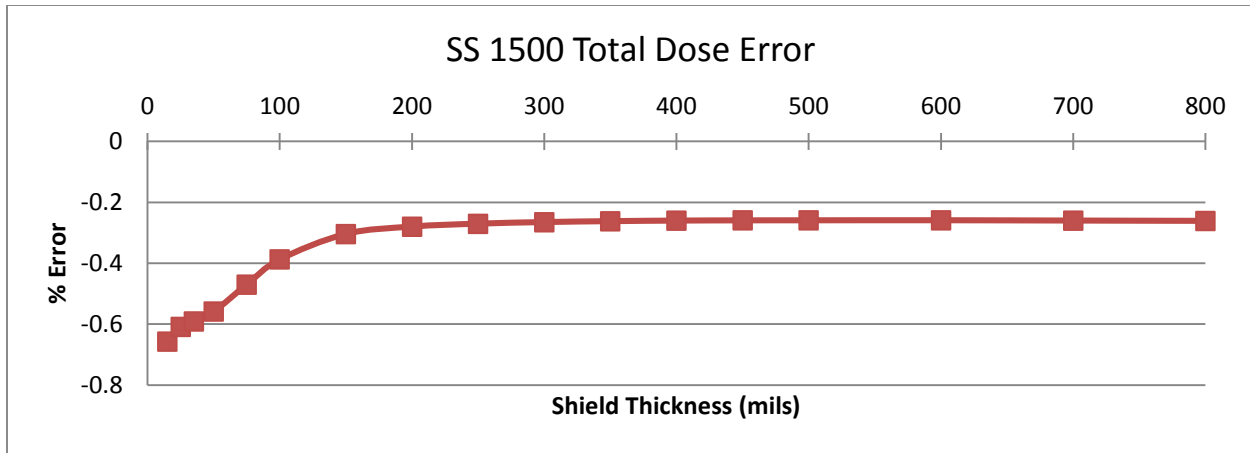


Figure 31. Sun-Synchronous orbit at 1500 km total dose error.

3.11 Mid-Inclined LEO at 400 km

This mid inclined LEO has an altitude of 400 km and an inclination of 51.46 deg. This orbit has reasonable agreement between the static tables and the AE9/AP9 models. The electrons have an error between 4% and 6% for all energy levels below for 4 MeV where it rises to a maximum of 14%. The protons have an error less than 6% at all energy levels. The total dose error is very consistent between 4% and 5%. Figure 32, Figure 33, and Figure 34 show the error between the static tables and the AE9/AP9 models for electron fluence, proton fluence, and total dose for this sun synchronous orbit respectively.

Not shown in Figure 33 is the case for protons at 1200 MeV. In this case, the AP9 model reports a fluence count while the static tables do not, resulting in a 100% error. The fluence reported by the AP9 model for 700 MeV protons is $1e6$ while the fluence for 1200 MeV protons is $5.5e3$ representing a steep drop off in the particle environment between these two energy levels.

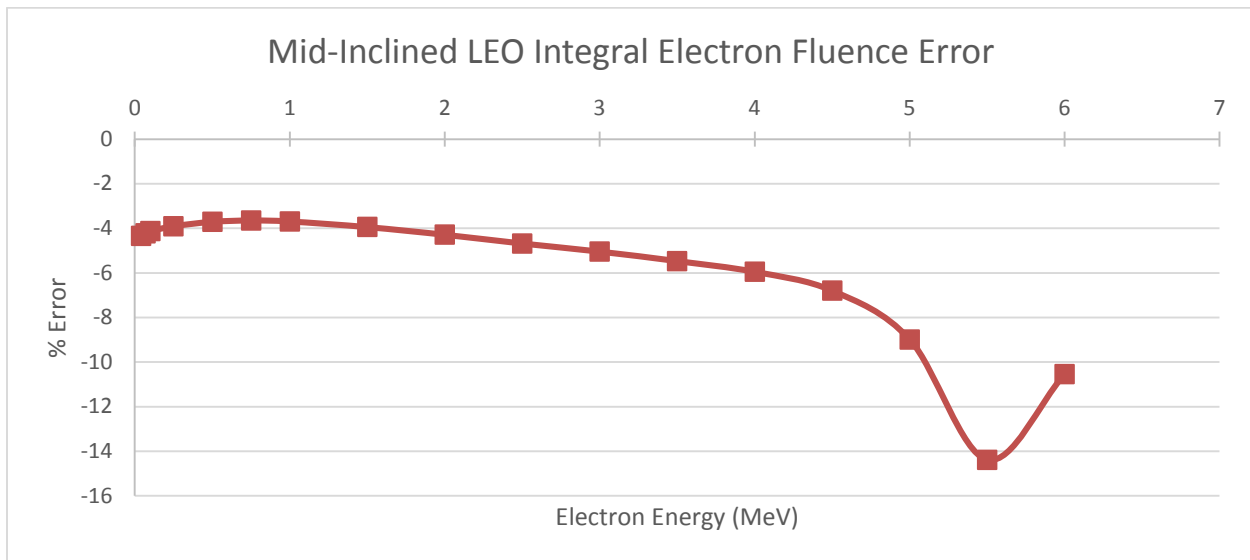


Figure 32. Mid-Inclined LEO at 400 km integral electron fluence error.

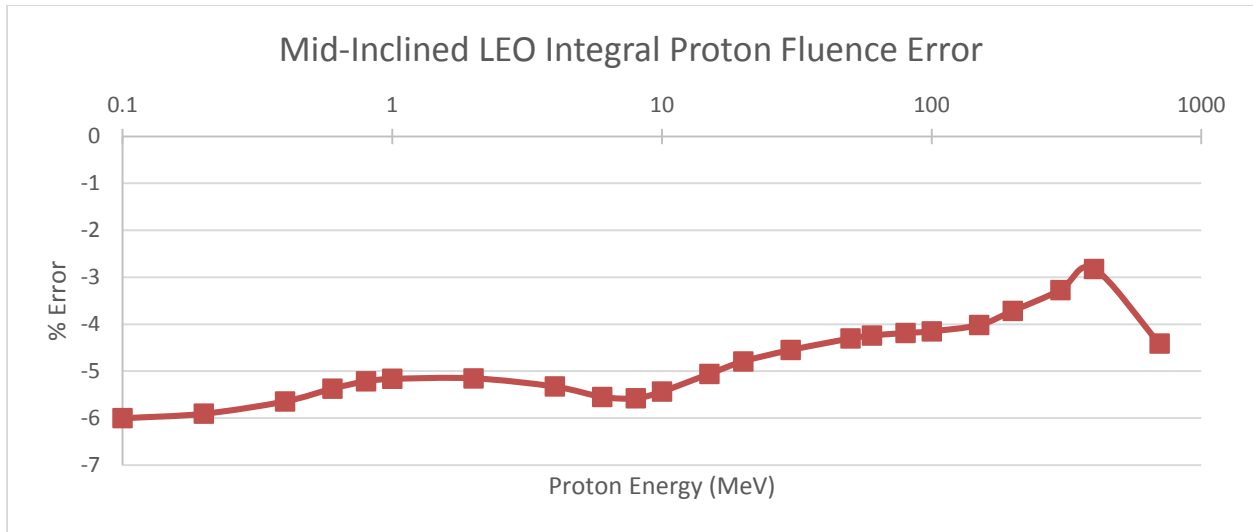


Figure 33. Mid-Inclined LEO at 400 km integral proton fluence error.

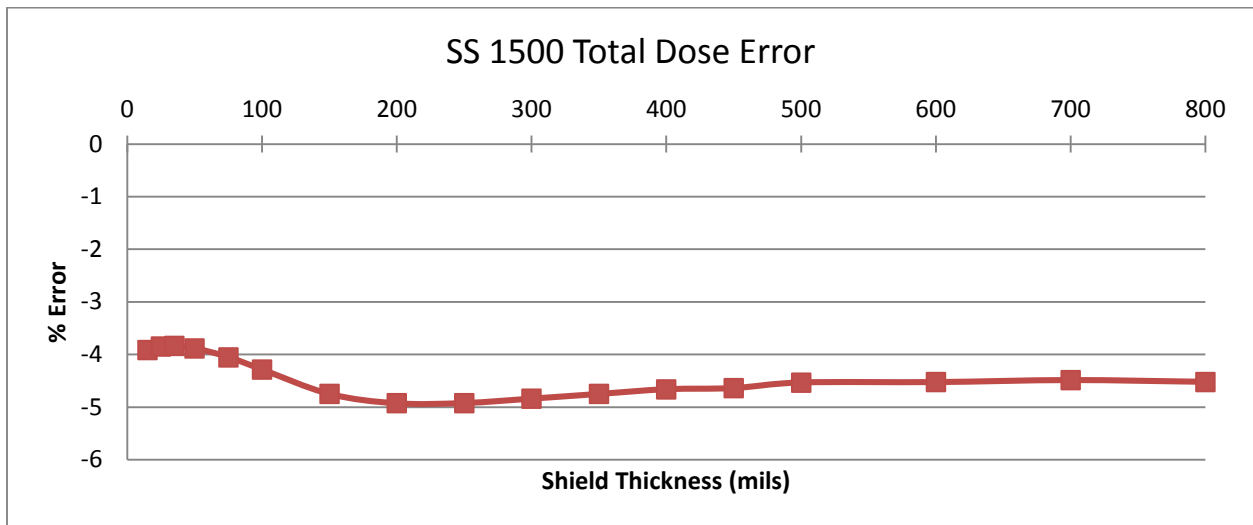


Figure 34. Mid-Inclined LEO at 400 km total dose error.

4. Conclusion

The static tables seem to have very good agreeability with the AE9/AP9 models for most of the orbits looked at. Generally, the errors found were less than 5%. Of the eleven orbits studied, the static tables overestimated the environment only for the GIO, Tundra, Molniya, and PNT orbits. For the remaining seven orbits, the static tables underestimated the environment.

In many of the cases looked at, there was a sudden increase in errors at the highest energy levels present; also, some orbits had fluences reported by the AE9/AP9 models that were not reported by using the static tables. It is worth noting that in instances of large disagreement between the two methods, or instances where the AE9/AP9 model showed a fluence where the tables did not, there was generally a significant difference in integral fluence between the energy levels surrounding the discrepancies.

Due to the high amount of agreeability across all orbits studied, it can be concluded that the method of generating static tables of AE9/AP9 model data is viable, and the static tables provide an alternative to running the AE9/AP9 software as long as an approximately $\pm 5\%$ error is acceptable to the user.

Because both the short (hourly) and long (seasonal) time variations of the mean model were accounted for in the averaging of the data tables, it is unknown why these discrepancies still exist. It may be possible that the fidelity of these data tables was insufficient in the three spacial dimensions to properly capture some of the finer details in regions of the radiation environment where there was rapid spacial change. The use of a geodetic coordinate system was selected because it is easy to work in for the spherical space around Earth, however it has limitations. Latitude and longitude resolution is good close to Earth, but as altitude increases the amount of physical distance from one longitude or latitude point to the next becomes significant, which may be one source of pixilation error.

Another approach for these data tables would be to increase the number of dimensions captured in the data tables from three to four and incorporating a time variation. In this way, a more accurate representation of the radiation environment might be captured and the static tables might be usable for mission durations shorter than one year. Doing this, however, would increase the file size of the data table by a multiplier equal to the number of time steps included. While file storage may not be an issue, load time and working memory size might be prohibitive.

5. References

1. Ginet, G. P., T. P. O'Brien, S. L. Huston, W. R. Johnston, T. B. Guild, R. Friedel, C. D. Lindstrom, C. J. Roth, P. Whelan, R. A. Quinn, D. Madden, S. Morley, Yi-Jiun Su, "AE9, AP9 and SPM: New Models for Specifying the Trapped Energetic Particle and Space Plasma Environment," *Space Sci Rev*, 179:579-615 (2013)
2. Stodden, D. Y. and G. D. Galasso, "Space System Visualization and Analysis Using the Satellite Orbit Analysis Program (SOAP)," *Proceedings of the 1995 IEEE Aerospace Applications Conference*, Aspen, Colorado, 4-11 February 1995
<http://ieeexplore.ieee.org/stamp/stamp.jsp?arnumber=00468892>
3. "Earth's Seasons," *Earth's Seasons*. USNO, n.d. Web. 05 Jan. 2015.
<http://aa.usno.navy.mil/data/docs/EarthSeasons.php>

Generating Lookup Tables from the AE9/AP9 Models

Approved Electronically by:

Richard H. Gong, SYSTEMS
DIRECTOR
SPACE & GROUND
DEVELOPMENTAL
PLANNING & PROJECTS
SYSTEMS PLANNING
ENGINEERING & QUALITY

Robert J. Minnichelli, PRINC
DIRECTOR
ARCHITECTURE & DESIGN
SUBDIVISION
SYSTEMS ENGINEERING
DIVISION
ENGINEERING &
TECHNOLOGY GROUP

Andrew B. Dawdy,
GENERAL MANAGER
DEVELOPMENTAL
PLANNING &
ARCHITECTURES
SYSTEMS PLANNING
ENGINEERING & QUALITY

Rand H. Fisher, SR VP
SPEQ
SYSTEMS PLANNING
ENGINEERING & QUALITY

Technical Peer Review Performed by:

Jeffrey Padin, MANAGER-
ENGRG
VEHICLE CONCEPTUAL
DESIGN SECTION
VEHICLE CONCEPTS DEPT
ENGINEERING &
TECHNOLOGY GROUP

T Paul P. O'Brien, RES
SCIENTIST
AVIR MAGNETOSPHERIC &
HELIOSPHERIC SCI
SPACE SCIENCES
DEPARTMENT
ENGINEERING &
TECHNOLOGY GROUP

Joseph E. Mazur, ASSOC
DIRECTOR
AVIR MAGNETOSPHERIC &
HELIOSPHERIC SCI
SPACE SCIENCES
DEPARTMENT
ENGINEERING &
TECHNOLOGY GROUP

External Distribution

REPORT TITLE

Generating Lookup Tables from the AE9/AP9 Models

REPORT NO.

TOR-2015-00893

PUBLICATION DATE

June 16, 2015

SECURITY CLASSIFICATION

UNCLASSIFIED

Scott Messenger
University of Maryland
smessel@umbc.edu

Nabil Attallah
SMC/ADXM
nabil.attallah@us.af.mil

Joseph Wang
University of Southern
California
josephjw@usc.edu

Roberta Ewart
SMC/AD
roberta.ewart@us.af.mil

Lt Col Alesandro Smith
SMC/ADXR
alesandro.smith@@us.af.mil

Douglas Brown
SMC/ADYT
douglas.brown.35@us.af.mil

Maj Lyle Rountree
SMC/ADYI
stewart.rountree@us.af.mil

James Taniguchi
SMC/ADX
james.taniguchi@us.af.mil

Trevor Dobson
Northrop Grumman
Trevor.Dobson@ngc.com

Vince Caponpon
SMC/ADXC
vincent.caponpon@us.af.mil

Michael Gruntman
University of Southern
California
mikeg@usc.edu

APPROVED BY _____
(AF OFFICE)

DATE _____